HHS Public Access

Author manuscript

Brain Topogr. Author manuscript; available in PMC 2021 March 01.

Published in final edited form as:

Brain Topogr. 2020 March ; 33(2): 221–237. doi:10.1007/s10548-020-00757-6.

EEG functional connectivity is a weak predictor of causal brain interactions

Jord JT Vink, MSc[1], **Deborah CW Klooster, PhD**[2,3], **Recep A. Ozdemir, PhD**[4], **M Brandon Westover, MD, PhD**[5], **Alvaro Pascual-Leone, MD, PhD**[6,7], **Mouhsin M Shafi, MD, PhD**[4]

[1]Biomedical MR Imaging and Spectroscopy Group, Center for Image Sciences, University Medical Center Utrecht and Utrecht University, Heidelberglaan 100, 3584CM, Utrecht, The Netherlands [2]Department of Electrical Engineering, Eindhoven University of Technology, 5612AZ, Eindhoven, The Netherlands [3]Deparment of Neurology, University Hospital Ghent, Corneel Heymanslaan 10, 9000 Ghent, Belgium [4]Berenson-Allen Center for Noninvasive Brain Stimulation; Department of Neurology, Harvard Medical School and Beth Israel Deaconess Medical Center, 330 Brookline Avenue, Boston, MA 02215, USA [5]Massachusetts General Hospital, 55 Fruit St, Boston, MA 02114, USA [6]Hinda and Arthur Marcus Institute for Aging Research and the Center for Memory Health, Hebrew SeniorLife. Department of Neurology, Harvard Medical School, Boston, MA, USA [7]Institut Guttman, Universitat Autonoma de Barcelona, Camí Can Ruti, s/n, 08916 Badalona, Barcelona, Spain

Abstract

In recent years there has been an explosion of research evaluating resting-state brain functional connectivity (FC) using different modalities. However, the relationship between such measures of FC and the underlying causal brain interactions has not been well characterized. To further characterize this relationship, we assessed the relationship between EEG resting state FC and propagation of transcranial magnetic stimulation (TMS) evoked potentials (TEPs) at the sensor and source level in healthy participants. TMS was applied to 6 different cortical regions in 10 healthy individuals (9 male; 1 female), and effects on brain activity were measured using simultaneous EEG. Pre-stimulus FC was assessed using 5 different FC measures (Pearson's correlation, mutual information, weighted phase lag index, coherence and phase locking value). Propagation of the TEPs was quantified as the root mean square (RMS) of the TEP voltage and

Corresponding author: Jord Vink; j.j.vink-5@umcutrecht.nl; phone: 0031634959811; Heidelberglaan 100, 3584CX, Utrecht, The Netherlands.

Conflicts of interest

APL serves on the scientific advisory boards for Starlab Neuroscience, Neuroelectrics, Constant Therapy, Cognito, and Neosync; and is listed as an inventor on several issued and pending patents on the real-time integration of transcranial magnetic stimulation with electroencephalography and magnetic resonance imaging.

The content is solely the responsibility of the authors and does not necessarily represent the official views of Harvard Catalyst, Harvard University and its affiliated academic health care centers, the National Institutes of Health, or the Sidney R. Baer Jr. Foundation.

current source density (CSD) at the sensor and source level, respectively. The relationship between pre-stimulus FC and the spatial distribution of TEP activity was determined using a generalized linear model (GLM) analysis. On the group level, all FC measures correlated significantly with TEP activity over the early (15–75ms) and full range (15 – 400ms) of the TEP at the sensor and source level. However, the predictive value of all FC measures is quite limited, accounting for less than 10% of the variance of TEP activity, and varies substantially across participants and stimulation sites. Taken together, these results suggest that EEG functional connectivity studies in sensor and source space should be interpreted with caution.

Keywords

connectomics; EEG; functional connectivity; TMS; evoked potentials; propagation

1. INTRODUCTION

In recent years, it has become apparent that normal brain function results from activity across distributed networks of brain regions that engage in complex, dynamic interactions. Consequently, brain connectomics has emerged as a major area of investigation(van den Heuvel and Hulshoff Pol 2010; Sakkalis 2011). Brain connectivity is generally studied in the task-free resting state using modalities such as electroencephalography (EEG), magnetoencephalography (MEG), and functional Magnetic Resonance Imaging (fMRI). The evaluation of functional connectivity (FC) is used to understand brain function in healthy individuals and in patients with a wide range of neuropsychiatric diseases ranging from stroke to schizophrenia(Micheloyannis et al. 2006; Greicius 2008; Grefkes and Fink 2011). In FC studies, two regions are said to be functionally connected if their activity is statistically correlated, and this FC is often interpreted to indicate causal interactions between those brain regions. However, the fundamental assumption that resting-state FC reflects causal brain interactions has not been adequately verified. Specifically, there is limited evidence that FC between two regions is related to direct electrophysiological interactions between them.

A problem in the study of EEG and MEG connectivity is the appropriate level of analysis. Specifically, EEG signals are recorded from the scalp, and reflect the superposition of the signals originating from the entire cortical surface. Consequently, some studies suggest that sensor-space analyses are sub-optimal for the assessment of causal interactions between brain regions(Mahjoory et al. 2017). However, the localization of the underlying brain signals is fundamentally ambiguous because the inverse problem of identifying the cortical sources that generate the scalp EEG signals is “ill-posed”, with an infinite number of possible solutions. Consequently, a wide variety of different methods exist for estimating source solutions, often with varying results for the same scalp recording(Becker et al. 2015; Mahjoory et al. 2017). Thus, despite the intensive interest in FC, the relationship between these different measures of FC and the underlying neurophysiological interactions remains poorly understood(Chen et al. 2013), at the sensor and source level. An additional problem in the interpretation of FC is the variety of FC measures that are used in the literature. These

measures capture different aspects of the underlying brain signal, and thus produce different connectivity patterns(David et al. 2004)(Wendling et al. 2009).

Previous efforts have tried to shed light on the relationship between functional connectivity and the spatial distribution of evoked activity by combining fMRI and invasive stimulation/recording techniques in macaques (Matsui et al. 2011) and human patients with epilepsy (Keller et al. 2011), intracranial EEG recording and stimulation in epilepsy patients(Hebbink et al. 2019), or optogenetic stimulation and intracranial EEG recording in macaques(Yazdan-Shahmorad et al. 2018). However, these studies only investigated a small sample, often focused primarily on connectivity within the primary somatomotor network (which is known to exhibit relatively stable connectivity), and are necessarily limited in their scope insofar as these techniques cannot be applied in human populations without implanted intracranial EEG electrodes (which are currently limited to patients with refractory epilepsy).

Transcranial Magnetic Stimulation (TMS) uses electromagnetic induction to directly stimulate a targeted cortical region. Although stimulation is applied focally, the effects of TMS do not remain local (in the targeted cortical region), but spread to other brain regions(Bestmann et al. 2005; Shafi et al. 2014; Vink et al. 2018), with the propagation pattern presumably determined by connectivity between the stimulated region and other brain areas(Rahman et al. 2013). When combined with EEG, TMS can be used to assess local and distant brain responses to controlled perturbations. Consequently, TMS in combination with EEG can be used to test the hypothesis that resting-state FC reflects electrophysiological interactions between brain regions. Recent work has already indicated that such a relationship exists for hemodynamic data, by comparing resting state fMRI FC of the DLPFC with the spatial distribution of activity evoked at the DLPFC(Hawco et al. 2018). To the best of our knowledge, this relationship has not yet been investigated using electro-cortical oscillations as measured with concurrent TMS-EEG.

To test whether the relationship between resting-state FC and causal brain interactions also exists for electro-cortical oscillations, we acquired concurrent TMS-EEG data of ten healthy volunteers. Because of the above mentioned limitations, we performed a broad study, using EEG in sensor- and source-space and quantifying FC with multiple measures. Specifically, we hypothesized that sensor- and source-level measures of EEG resting-state FC predict the spatial distribution of TMS-evoked potentials (TEPs).

2. MATERIALS AND METHODS

2.1 Data acquisition

TMS-EEG data was recorded from 11 healthy right-handed participants. Written informed consent was provided by all and the experimental procedure was approved by the Committee for Clinical Investigations of Beth Israel Deaconess Medical Center. One participant was excluded from the study because of TMS intolerance (excessive discomfort with TMS-induced scalp muscle contractions), leaving 10 participants (mean age: 38 (20–63 years); 9 males, 1 female; all right-handed) for data analysis.

EEG was recorded with a 60-channel TMS-compatible eXimia EEG system (Nexstim, Helsinki, Finland). The reference and ground electrodes were placed on the forehead. EEG signals were recorded at 1450 Hz with 16-bit resolution, and were band-pass filtered between 0.1 and 500 Hz. Two additional sensors were used to record the electro-oculogram (EOG). Electrode impedance was kept below 5kOhms.

Single biphasic pulses of TMS were administered via a Nexstim eXimia stimulator using a figure-of-eight coil (mean diameter 59 mm, outer diameter 70 mm). Stimulation was applied using MRI-guided neuronavigation to six different anatomically defined target sites in each individual (Fig. 1A): the left and right dorsolateral prefrontal cortex (DLPFC), primary motor cortex (M1) and parietal cortex (PAR). The DLPFC target was anatomically defined as a point on the superior aspect of the middle frontal gyrus, 1–2 cm anterior to the premotor gyrus. The M1 target was the motor hotspot, defined as the point that produced the largest EMG response in the first dorsal interosseous (FDI) muscle. The parietal target was the posterior half of the angular gyrus, 1–2 cm below the intraparietal sulcus. These sites were selected because: (1) The targets in the middle frontal gyrus and angular gyrus are part of the prefrontal and parietal association cortices respectively, with relatively complex connectivity across participants (Mueller et al, 2013, Neuron), whereas M1 is part of the somatomotor network with more stereotyped connectivity; (2) These sites are generally part of distinct functional networks (middle frontal gyrus - frontoparietal control network; Angular – DMN; M1 – somatomotor network) and thus should have distinct functional connectivity. The TMS coil was oriented so that the direction of the TMS electrical field was oriented perpendicular to the orientation of the target gyrus, with the coil handle oriented posterolaterally to the site of stimulation. For example, for left M1, the coil handle was oriented posteriorly at approximately 45% to the mid-sagittal line. Stimulation was applied at 120% resting motor threshold (RMT), defined as the lowest intensity at which TMS to M1 induced a motor evoked potential (MEP) in the contralateral FDI muscle of more than 50 μV in 5 out of 10 trials. In addition, all participants received sham stimulation, in which the TMS coil was positioned over the left M1 while rotated 90 degrees (with the plane of the coil perpendicular rather than parallel to the scalp), so that the TMS coil rested on the participant's scalp on edge. This was done in order to obtain the sham-evoked potential, which was used to control for auditory and some of the somatosensory sensations associated with the TMS pulse(Lisanby et al. 2001). Participants received between 80 and 110 single pulses to each site, with a random inter stimulus interval of 4 to 6s to avoid conditioning. Participants were seated comfortably in a reclining chair with their eyes open and were asked to look straight ahead at a fixation point, while TMS was delivered according to the guidelines and recommendations for TMS endorsed by the International Federation for Clinical Neurophysiology(Rossi et al. 2009).

2.2 Preprocessing

Data analysis was performed with custom scripts, EEGLAB 14.1.2b(Delorme and Makeig 2004), Brainstrom(Tadel et al. 2011) and Fieldtrip(Oostenveld et al. 2011) in the Matlab R2015a environment (MathWorks Inc., USA). An ICA-based cleaning procedure was used to remove artifacts from the pre- and post-stimulus segments(Rogasch et al. 2014). The data were divided into pre- and post-stimulus segments of −2900 to −400ms and −500 to

1000ms, respectively, with TMS pulse delivery at 0ms (Fig. 1A). An average of 3.4 (range: 1–6) and 3.3 bad channels (range: 0–6) were removed and interpolated from the pre- and post-stimulus data, respectively. Pre- and post- stimulus segments were baseline corrected on −3300 to −2500ms and −900 to −100ms, respectively. All data were baseline-corrected to minimize the difference between the two preprocessing pipelines. The TMS artifact in the post-stimulus segment was zero-padded from 0 to 14ms. A semi-automated procedure was used to detect and remove noisy epochs in all data(Rogasch et al. 2014), resulting in the removal of an average of 18 pre-stimulus epochs (range: 3–50) and 14 post-stimulus epochs (range: 5–41), leaving an average of 80 pre-stimulus epochs (range: 50–112) and 83 post-stimulus epochs (range: 65–116). The TMS-evoked exponential decay artifact was removed from the post-stimulus segment in a first round of ICA. Thereafter, Gaussian interpolation was used to fill in the missing data from 0 to 14ms. Both the pre- and post-stimulus segments were filtered with a bandpass filter of 1 to 100Hz and a bandstop filter of 55 to 65Hz using a fourth-order Butterworth filter with forward and backward filtering. Both segments were referenced to the average reference and then subjected to another round of ICA in which blink artefacts, muscle artefacts and other noise related artefacts were removed. After the cleaning procedure, an average of 20 ICA components (range: 12 – 26) were removed from the pre-stimulus data, and 16 ICA components (range: 8 – 24) were removed from the post-stimulus data.

Individual electrode data, topoplots from −50 to 300ms around stimulation with intervals of 10ms, and the global mean field potential (GMFP), were visually inspected by an experienced investigator (MMS) for the presence of non-physiological activity. The preprocessing procedure was repeated in case of non-physiological activity.

Volume conduction has been shown to affect functional connectivity in scalp level EEG data (Mahjoory et al. 2017). To minimize any potential confounding effects of volume conduction, we also evaluated the relationship between functional connectivity and evoked activity data using the surface laplacian reference(Perrin et al. 1989). For this analysis, the data was rereferenced to the surface laplacian reference after completing the aforementioned preprocessing procedure.

2.3 Source Analysis

The relationship between functional connectivity and evoked activity was also assessed at the source level. EEG source imaging (ESI) was performed (Figure 1B) using BrainStorm(Tadel et al. 2011). Individual three-layer head models were generated based on individual anatomical MRI data using OpenMEEG (Gramfort et al. 2010). The cortical surface was sampled at 15,000 vertices, to minimize computational load while maintaining accuracy of individual brain morphology. A current dipole was assigned to each of the vertices of the cortical surface. The dipoles are oriented perpendicular to the cortical surface, so that they align with the cortical pyramidal neurons which are presumed to generate most of the EEG activity. The coordinates of the EEG electrodes (as captured using the neuronavigation system) were used to position them within the individual head model. OpenMEEG, which is based on a symmetric boundary element method, was used to compute the leadfield matrix with the default parameter settings. The noise covariance

matrix was computed from −2900 to −2400ms and from −500 to 0ms of the pre- and post-stimulus segments, respectively. Subsequently, the linear L2-minimum norm estimates (wMNI) algorithm was used to solve the ill-posed inverse problem(Baillet et al. 2001). We selected 42 parcels from the Desikan-Killiany atlas(Desikan et al. 2006) for analysis (a table of included parcels is shown in Online Resource 1), disregarding the deeper parcels. We disregarded deeper parcels because the accuracy of source estimation is controversial for deeper structures(Whittingstall et al. 2003), although advances in the detection of activity in deeper sources has been made(Seeber et al. 2019). As the dipoles are oriented perpendicular to the cortical surface, the average signal of a parcel which contains opposing gyral surfaces cancels out. Therefore, the dominant dipole orientation of each parcel was determined by means of singular value decomposition of the orientations of all dipoles within the parcel. The time-series of the dipoles that were not aligned with the dominant orientation of the parcel were flipped. Subsequently, the source-space time-series were averaged to obtain a single time-series for each parcel.

2.4 Data analysis

We set out to identify whether resting state FC measured prior to the delivery of a TMS-pulse predicts the spatial distribution of the TEP, by introducing these variables in a generalized linear model (GLM). The pre- and post- stimulus scalp and source segments data were filtered with second-order Butterworth filters to organize the data into 5 frequency bands: broadband (1 – 80Hz), theta (4 – 8Hz), alpha (8 – 12Hz), beta (12 – 30Hz) and gamma (30–80Hz) band. The analyses were based on broadband data unless specified otherwise. In addition to pre-stimulus FC and post-stimulus TEP activity, we used a volume conduction control, sham-EP and pre-stimulus RMS as nuisance regressors in the GLM analysis. The inputs and output are shown schematically in Figure 1C and 1D, for sensor and source space respectively. Calculation of the GLM inputs is described in more detail in sections 2.4.1 to 2.4.4. GLMs were constructed for each participant and stimulation site separately. The GLMs were fitted using a gamma distribution (with reciprocal link function), due to the non-negative nature of the outcome variable (the RMS of the TEP). Calculation of the input and response variables is described in more detail below. The input variables were calculated for the sensor- and source-level data, unless explicitly mentioned otherwise in the sections below.

2.4.1 Resting state functional connectivity maps—The MRI-guided navigation system registers the position of the TMS coil isocenter with respect to the positions of the EEG electrodes; the TMS target electrode was defined as the EEG electrode or the parcel closest to the TMS coil isocenter. The FC strength between the TMS target electrode (seed) and all the other channels (and the stimulated parcel and all other parcels in the source analysis) was calculated for each pre-stimulus epoch, individually. The FC values for the individual epochs were averaged together to obtain a single FC map per participant and stimulation site. We included 5 different FC measures in our analysis, producing 5 FC maps per stimulation site and participant (Fig. 3). We selected weighted phase lag index (wPLI; (Vinck et al. 2011)), phase-locking value (PLV; (Lachaux et al. 1999)), magnitude squared interchannel coherence (ICC;(Rosenberg et al. 1989)), Pearson's correlation (R) and mutual information (MI;(Magri et al. 2009)) for our FC analysis. Because concerns have been raised

on the reliability of directed connectivity measures(de Steen et al. 2016), we restricted our analysis to non-directional measures of connectivity. We included a diverse group of FC measures, as MI and C are time-based FC measures, wPLI and PLV are phase-based FC measures and the ICC is a power-based FC measure.

All FC measures were calculated using Fieldtrip(Oostenveld et al. 2011). FC measures were calculated for the interval of −2900 to −400ms, with TMS pulse delivery at 0ms, to minimize the effect of edge artefacts. MI was calculated with 13 bins and equipopulated binning. Both the wPLI and the ICC were determined from cross power spectral density data, which was calculated with a single taper with 0.5Hz smoothing. The formulae for the connectivity and evoked activity measures are provided in Table 1.

Pearson's correlation and wPLI potentially exhibit negative FC, while the other measures are positive by default. To maintain consistency we decided to calculate the absolute value of all FC values. However, negative FC potentially indicates inhibitory connectivity, which might not result in evoked activity. Therefore, we also investigated whether the predictive value of Pearson's correlation and wPLI increased when negative FC values were excluded from analysis.

2.4.2 Evoked activity maps—For all channels, the post-stimulus epochs of active and sham TMS data were averaged to obtain the average TEP and sham-EP, respectively. TEP and sham-EP activity maps were obtained by calculating the root mean square (RMS) voltage and the current source density (CSD) of the EP in sensor and source space, respectively. The RMS voltage and CSD were calculated for the early interval (15 to 75ms; Fig 4) and the full interval (15 to 400ms) of the TEP. As it is possible that TEP activity beyond 75ms is not directly related to activation of the stimulated site, but rather related to activation of remote regions, we specifically evaluated the early time window (from 15 – 75ms) to identify whether functional connectivity only captures TEP propagation directly from the stimulated target. Additionally, the activity beyond the first 75ms of the TEP may include peripherally evoked potentials (PEPs)(Freedberg et al. 2019), contaminating our analysis.

2.4.3 Nuisance variables—We included three nuisance variables in the analysis: a volume conduction control, the spatial distribution of the sham-EP and the pre-stimulus RMS voltage or CSD.

In the sensor space analysis, a volume conduction control was determined by calculating the absolute Euclidean distance between the TMS target electrode and all the other electrodes, based on the coordinates provided by the navigation system. For the source space analysis, cross-talk functions (CTFs) were used to estimate volume conduction effects between sources(Hauk and Stenroos 2014). The volume conduction control was included as a nuisance regressor to correct for a spurious relationship between FC and TEP activity due to shared volume conduction effects. As an additional control to ensure that volume conduction was not responsible for our results, we also repeated our analysis using EEG data with a surface laplacian reference (in sensor space only).

The spatial distribution of the sham-EP was included in the GLM analysis as a nuisance regressor in order to control for confounding evoked activity which is not directly related to activation of the stimulation target (e.g. the PEPs).

Pre-stimulus RMS was included to correct for baseline differences in signal strength across electrodes. Pre-stimulus RMS was determined between −250 and −50ms with respect to TMS pulse delivery at 0ms.

2.5 Statistics

The proportion of variance of TEP activity $\left(R^2_{total}\right)$ explained by all input variables was calculated for each participant at each stimulation site. The R^2_{total} was corrected for the variance explained by the nuisance regressors $\left(R^2_{nuisance}\right)$, leaving the proportion of variance of the TEP explained by FC only $\left(R^2_{FC}\right)$.

$$R^2_{total} = R^2_{FC} + R^2_{nuisance}$$

Random permutation statistics was used to determine significance on the individual level. This was done by calculating 2,000 random permutations of the rank order of the FC map for each analysis. We randomly permutated the rank order to maintain a biologically feasible range of FC values. The randomly permutated FC map was used in the previously described GLM analysis to calculate a random distribution of R^2_{FC} values. On the individual level, a p-value was calculated for each participant and stimulation site, separately, using the following formula:

$$p = \frac{\left(amount\ of\ permutations > R^2_{FC}\right) + 1}{total\ amount\ of\ permutations + 1}$$

To determine significance on the group-level, the R^2_{rsFC} values of all participants and stimulation sites were averaged together for each permutation to obtain a group-level distribution of R^2_{FC} values. Next, a group-level p-value was calculated by calculating the amount of permutations that exceed the mean R^2_{FC} using the previously described formula. The family wise error (FWE) rate was used to correct the alpha level of different analyses for multiple comparisons.

A Kruskal Wallis test was performed to test whether the investigated FC measures are equally informative on TEP activity. In case of significance, multiple Mann Whitney U tests were performed to determine whether the measure which explained most variance was significantly more informative than the other measures. Finally, a paired t-test was used to determine whether combining the FC measures in a single analysis improved the predictive value with respect to the single best-performing FC measure (FC measure with the highest mean R^2_{FC}). As the inclusion of more variables to the GLM increases the proportion of

variance explained, random permutations of the single FC measure were added to the GLM analysis of the individual FC measure to match the number of variables in the GLM analysis of the combination of FC measures.

Further statistical testing was restricted to Pearson's correlation based FC (R-FC). One-sided paired t-tests were also used to determine whether the predictive value of R-FC improved when the analysis was restricted to the early interval of the TEP at the sensor and source level, as might be expected given the recent literature suggesting that later TEP activity may be contaminated by peripheral-evoked potentials(Biabani et al. 2019)(Freedberg et al. 2019). A one sided paired t-test was used to investigate whether moving from sensor space to source space increased the predictive value of R-FC, as recent literature indicates a greater reliability of source-space connectivity(Mahjoory et al. 2017). Kruskal-Wallis tests were used to identify whether the informative value of R-FC varied between stimulation locations and frequency bands. In case of significance, multiple Mann Whitney U tests were performed to determine whether a single stimulation location or frequency band outperformed the others.

3. RESULTS

Time series of the sham-corrected TEPs elicited at the 6 different stimulation sites and the sham EP are shown for a representative participant (Fig. 2; time series and topoplots of the uncorrected, sham-EPs and sham-corrected TEPS are presented in Online Resource 2, 3 and 4, respectively). The sham-corrected TEP was calculated by subtracting the sham-EP time series from the TEP time series. Topoplots were constructed from the time series data at different time points, which were based on peaks in the GMFP of the EP. The topoplots show a dipole originating at the stimulation site which spreads to other regions. For example, the data obtained during stimulation of the LM1 shows a dipole near Cz at 28ms, which shifts posteriorly at 88ms. The TEP data clearly shows a distinct spatial distribution of activity compared to the sham-EP data.

Figure 3 shows Pearson's correlation based FC maps at the sensor (Fig. 3A) and the source (Fig. 3B) level of a representative participant. The sensor level maps show the stimulated electrode which was used as a seed for the connectivity analysis. In the source level maps the stimulated parcel which was used as a seed for the connectivity analysis is indicated by a red beam. The sensor level connectivity maps show strong local connectivity near the stimulation site, as well as connected foci more distally (e.g. the RDLPFC shows functional connectivity with the contralateral DLPFC and the bilateral parieto-occipital regions). The source level connectivity maps show more focal and complex connectivity patterns with high site specificity.

Figure 4 shows evoked activity for stimulation of 6 different TMS targets and for sham stimulation at the sensor (Fig. 4A) and the source (Fig. 4B) level of the same participant. In the source level maps the stimulated parcel is indicated by a red beam. Both sensor and source level maps show evoked activity at the stimulated site and distant regions, with variability across stimulation sites. The site-specificity of the evoked response is more prominent at the source level.

3.1 Predictability

Our goal was to test the hypothesis that FC measures predict the spatial distribution of a TEP at the source and sensor level. We found that all of the resting state FC measures deliver a significant contribution to the explained variance of early (15 to 75ms) and full (15 to 400ms) TEP activity at both the sensor and source level, when corrected for nuisance regressors ($p < 0.05$, FWE corrected; Fig. 5).

The different FC measures performed equally well in the prediction of early (15–75ms) TEP activity at the sensor (Chi square = 2.36, p = 0.67, df = 4, 295) and the source level (Chi square = 0.54, p = 0.97, df = 4, 295). Adding all FC measures together into the model significantly improved the predictive value with respect to the single best FC measure (highest mean R^2_{rsFC}) at the sensor level (t-stat = 7.61, $p < 0.05$, df = 59), while this was not the case at the source level (t-stat = 1.15, p = 0.25, df = 59).

The different FC measures were also equally predictive of full TEP activity at the sensor (Chi square = 1.73, p = 0.79, df = 4, 295) and source level (Chi square = 2.99, p = 0.56, df = 4, 295). Combining all FC also significantly improved the predictive value at the sensor (t-stat = 2.79, $p < 0.05$, df = 59) and the source level (t-stat = 3.29, $p < 0.05$, df = 59). The results for the surface laplacian data were not substantially different from the average reference and are therefore restricted to Online Resource 5.

We also investigated whether the predictive value of Pearson's correlation and wPLI increased when negative FC values were removed from the analysis. We found that removing negative FC values from the analysis did not consistently improve the predictive value of these measures at either the sensor and source level (see Online Resource 6).

As all measures performed equally well, we restricted subsequent detailed description to R-FC. We found that R-FC is significantly more predictive of early (15–75ms) TEP activity compared to full (15400ms) TEP activity at the sensor level (t-stat = 2.69, $p < 0.05$, df = 59). Interestingly, this was not the case at the source level (t-stat = −0.12, p = 0.55, df = 59).

We hypothesized that the relationship between R-FC and TEP activity was strengthened by going from sensor to source space, as source-space connectivity has been shown to be more reliable(Mahjoory et al. 2017). However, the relationship between FC and the TEP was not significantly different between sensor and source space for the early TEP (t-stat = −0.68, p = 0.75, df = 59) or the full TEP (t-stat = 1.45, p = 0.08, df = 59).

As R-FC was more predictive of early TEP activity at the sensor level, and the predictive value did not increase when moving the analysis to source space, we restricted subsequent description to the relationship between R-FC and early TEP activity. The relationship between R-FC and early TEP activity was analyzed in more detail by investigating the different stimulation sites separately (Fig. 6). The relationship between R-FC and early TEP activity did not vary between stimulation sites at the sensor (Chi square = 8.07, p = 0.15, df = 5, 54) or source level (Chi square = 7.44, p = 0.19, df = 5, 54). We also investigated the relationship between frequency band specific FC and the spatial distribution of the broadband TEP (Fig. 7; Online Resource 7). R-FC was equally informative on the spatial

distribution of the broadband early TEP for all frequency bands in sensor (Chi square = 0.29, p = 0.99, df = 4, 295) and source (Chi square = 0.75, p = 0.94, df = 4, 295) space.

3.2 Variability

The relationship between FC and TEP activity was highly variable between participants and stimulation sites. On an individual level, R-FC correlated significantly with early TEP activity in less than half (24 out of 60) of cases at the sensor level and a fourth (15 out of 60 cases) of cases at the source level ($P < 0.05$, uncorrected). The variability can be observed clearly in Figure 8 (Online Resource 8). For example, at the sensor level, R-FC predicted early TEP activity in participants 1, 2, 4, 5 and 8 with stimulation of right M1, but did not predict early TEP activity in any of these participants with stimulation of left M1 (significant prediction only with participant 7).

4. DISCUSSION

Recent work has emphasized the importance of evaluating brain connectivity to understand normal brain function and neuropsychiatric diseases(Micheloyannis et al. 2006; Greicius 2008; Grefkes and Fink 2011), but the relationship between FC and the underlying causal interactions between brain regions is poorly understood. TMS allows for a controlled perturbation of activity in a given cortical target, and its local and distributed impact can be assessed by concurrent EEG recording. Consequently, the spread of the TEP may reflect causal interactions between the targeted brain region and the rest of the cortex. Therefore, we used TMS in combination with EEG to probe brain connectivity in human participants *in vivo*, and compared the resulting evoked activity with measures of EEG connectivity at the sensor and source level. We found that EEG FC patterns prior to delivery of a TMS pulse are weakly informative on the spatial distribution of evoked activity in response to the TMS pulse. This is in line with previous literature (Engel et al. 2001; Draguhn and Buzsaki 2004), suggesting that coordination of brain oscillatory activity plays a fundamental role in the organization of neuronal activity (and thereby information) across macroscopic brain regions. Specifically, the spatial distribution and magnitude of TMS-evoked activity can be partially predicted by resting-state FC measured prior to stimulation at the sensor and source level. Although the relationship between resting state FC prior to stimulation and the spatial distribution evoked activity was significant, we observed that the predictive value of all FC measures is poor (the proportion of the explained variance is less than 10%). The limited predictive value is likely related to the substantial variability across participants and stimulation sites.

In our study, we found that the relationship between individual EEG FC measures and evoked activity is weak and highly variable across individuals in both sensor and source space. Recent studies have already raised concerns about the utility of EEG connectivity measures in sensor space (Becker et al. 2015; de Steen et al. 2016; Mahjoory et al. 2017) and source space(Becker et al. 2015; Colclough et al. 2016). Our findings confirm these concerns, and should raise caution in the interpretation of studies involving EEG FC.

These findings also highlight the limitations of current functional connectivity analyses, and raise concern that current methods of characterizing EEG functional connectivity (at least

the methods explored in this paper) do not adequately characterize the nature and dynamics of interactions between different brain regions. However, we also found that when combining multiple measures, the predictive value increased significantly (with the exception of the prediction of early TEP activity in source space), suggesting that there may be some measure or a combination of measures that do capture the nature of neuronal interactions.

Because recent studies have raised concern that the TEP, particularly later components, may be contaminated by auditory and somatosensory evoked potentials(Biabani et al. 2019; Conde et al. 2019; Freedberg et al. 2019) and early TEP activity has been shown to be more consistent between participants(Salo et al. 2018), we specifically looked at the relationship between R-FC and the early interval (15 – 75ms) of evoked activity. At the sensor level, we found that R-FC is more predictive of the first 75ms of evoked activity compared to the full range (400 ms) of the TEP. Putting together these observations, we believe that our findings are consistent with the idea that early evoked activity is more specific to the stimulation site compared to late intervals (> 75ms) of the TEP, and therefore more likely to be caused directly by the TMS-induced electrical field. However, we also found that functional connectivity is equally predictive of early and full TEP activity at the source level. A possible explanation for this is our measure of the relationship between functional connectivity and TEP activity might be more strongly affected by the presence of PEPs at the sensor level compared to the source level. Specifically, although PEPs would clearly cause spurious activity in both sensor and source space, at the source level PEPs may occur primarily in the auditory and somatosensory cortices, two relatively well-defined and localized cortical parcels; however, due to volume conduction, activity in these brain regions might affect multiple electrodes (and thus our measure of the relationship between functional connectivity and TEP activity) at the scalp level.

We did not observe significant systematic differences in the strength of the relationship between R-FC and TEP activity between stimulation sites or frequency bands, suggesting that the predictive value of FC is consistent across brain regions and frequency bands. However, we did observe substantial variability in the relationship between resting state FC and TEP activity in individual participants. Specifically, for the same stimulation site, the relationship between R-FC and TEP activity was significant in some individuals but absent in others. This can be explained by variability in TEP activity patterns, which have been shown to become more variable at later intervals with respect to the stimulus delivery(Salo et al. 2018). Furthermore, this variability suggests that the degree to which measures of static resting-state FC capture causal brain interactions may not be consistent across individuals. This has also been reported by Hawco et al. (Hawco et al. 2018), who identified a relationship between resting state fMRI FC and the spatial distribution of TMS-evoked activity on the group level but also observed substantial variability between individuals. The cause for this inter-individual variability remains unclear but could potentially be explained by the fact that the chosen functional connectivity measures capture the fundamental nature of the interregional dynamics only in some participants, because of differences in intrinsic physiology, input-output relations, and network dynamics across participants. Other factors which are likely to contribute to the variability are differences in structural connectivity,

metabolism, brain state and neurochemistry between participants. Further studies are warranted to explore this important finding.

Our study has a number of limitations. Although we observed significant correlations between the investigated FC measures and the spatial distribution of evoked activity, the magnitude of the correlations was limited (mean R^2_{rsFC} values typically in the 0.03 – 0.09 range). There are a number of possible explanations for this.

First, we assessed the correlation between FC and the spatial distribution of a TEP in sensor space as a substantial amount of recent studies continue to analyze functional connectivity in sensor space(Nasseroleslami et al. 2017; Tóth et al. 2017; Hordacre et al. 2018). Therefore, we wanted to determine whether EEG FC analyses in sensor space are physiologically meaningful by comparing FC with TMS-evoked activity. However, concerns have been raised about the reliability of FC in sensor space(Mahjoory et al. 2017; O'Neill et al. 2017), as FC results have been shown to depend on the electrical reference(Nolte et al. 2008). In our study, we found that sensor-space connectivity does significantly predict the propagation of TMS-evoked potentials, but the correlation is weak and not entirely reliable across individuals; these findings are thus consistent with the aforementioned studies on the limited reliability of sensor-space FC. Another potential concern for sensor-space studies is spurious correlations induced by volume conduction. We made several attempts to minimize these effects, by analyzing the data using the surface laplacian reference and by including the distance between the electrodes as a nuisance regressor in our model (for the average reference data). It is possible that this did not entirely eliminate the problem. Because of the aforementioned concerns regarding sensor space FC, interest has shifted to source space.

However, source space analysis of FC introduces a second limitation, as source space analysis is complicated by the fact that the inverse problem (the identification of brain signals that generate sensor level EEG activity) is 'ill-posed', with an infinite number of possible solutions. Several methods exist to solve the inverse problem (one of which we investigated in this study), but the accuracy of these methods is not clearly defined, particularly in cases where multiple different cortical regions may be simultaneously activated (as might be expected to occur after TMS)(Becker et al. 2015), but also particularly with regard to resting-state functional connectivity analysis(Colclough et al. 2016). We found that the relationship between FC and evoked activity did not improve when moving to source space, demonstrating the complexity of the ill-posed inverse problem.

Third, we calculated the correlation between connectivity and the spatial distribution of TEPs by averaging the values obtained over multiple epochs, in part because this is how connectivity and TEPs are typically measured, and also because assessing the spatial distribution of TEPs on a single-trial level is not trivial. Therefore, our analysis assumed that the connectivity distribution and the spatial distribution of evoked activity, and the relationship between the two, are constant through the experiment. However, resting state FC has been shown to vary within sessions(Honey et al. 2009; Chang and Glover 2010; Handwerker et al. 2012; O'Neill et al. 2017), and this may therefore limit the absolute correlation between connectivity and the spatial distribution of the TEP. This is especially relevant for regions which exhibit strong connectivity dynamics, such as the bilateral

DLPFC and parietal cortices(Chen et al. 2015), which could potentially explain why these regions show a weaker relationship between FC and the spatial distribution of evoked activity in source space. A related possibility is that the TMS-evoked potential also varies substantially over time, perhaps due to state differences in the stimulated cortex affecting the TMS-evoked activity, as has been shown for the phase of ongoing rhythms affecting MEP amplitude with stimulation of M1(Schaworonkow et al. 2019).

Fourth, TMS also causes a somatosensory, auditory and motor response, which affects the observed spatial distribution of the TMS-evoked response(Conde et al. 2019; Rogasch et al. 2019). We attempted to control for this effect by including the sham-EP as a nuisance regressor in our model, but this might not be a perfect control. However, the cortical activity evoked by these nonspecific responses to TMS should be independent of the functional connectivity of the stimulated regions, and thus may also contribute to the relatively low explained variance.

Fifth, directed measures of connectivity are limited by the biological structure of neurons, which are restricted by directional distribution of activity. However, concerns have been raised regarding the reliability of EEG measures of directed connectivity, particularly at the sensor level (de Steen et al. 2016). We therefore decided to limit our analyses to non-directional measures of connectivity. In future work, directed measures should also be investigated.

Finally, TMS target regions for stimulation of the DLPFC and parietal targets were defined based on anatomical landmarks, rather than functional regions. However, the underlying functional regions vary in localization relative to macroscopic anatomical landmarks, especially for prefrontal and parietal regions(Yeo et al. 2011)(Goldman-Rakic 1987). It is possible that some variability exists in the functional regions that were targeted with TMS, providing a potential explanation for the observed variability in the relationship between FC and TEP activity between participants.

5. CONCLUSIONS

In summary, our results indicate that FC measures weakly predict the spatial distribution of subsequent TEPs at both the sensor and source level, and thus may contain some relevant causal information regarding brain networks and cortico-cortical interactions. However, the overall predictive power is limited, partly due to substantial variability across participants and stimulation sites. This variability raises concerns about whether studies characterizing EEG FC in cognitive function and disease states are physiologically meaningful. Further work is needed to better characterize the relationship between connectivity measures and the underlying cerebral dynamics.

Supplementary Material

Refer to Web version on PubMed Central for supplementary material.

Study funding/Acknowledgements

This study was supported by Citizens United for Research in Epilepsy (CURE). APL was partly supported by the Sidney R. Baer Jr. Foundation, the NIH (R01MH100186, R01HD069776, R01NS073601, R21NS082870, R21MH099196, R21NS085491, R21HD07616), and Harvard Catalyst | The Harvard Clinical and Translational Science Center (NCRR and the NCATS NIH, UL1 RR025758). MMS is supported in part by CURE and the NIH (R01 NS073601, R01MH115949). MBW receives funding from NIH-NINDS (1K23NS090900).

References

Baillet S, Mosher JC, Leahy RM (2001) Electromagnetic brain mapping. IEEE Signal Process Mag 18:14–30. 10.1109/79.962275

Becker H, Albera L, Comon P, et al. (2015) Brain source imaging : from sparse to tensor models To cite this version : HAL Id : hal-01190559 Brain source imaging : from sparse to tensor models

Bestmann S, Baudewig J, Siebner HR, et al. (2005) BOLD MRI responses to repetitive TMS over human dorsal premotor cortex. Neuroimage 28:22–29. 10.1016/j.neuroimage.2005.05.027 [PubMed: 16002305]

Biabani M, Fornito A, Mutanen T, et al. (2019) Sensory contamination in TMS-EEG recordings: Can we isolate TMS-evoked neural activity? Brain Stimul 12:473 10.1016/j.brs.2018.12.543

Chang C, Glover GH (2010) Time--frequency dynamics of resting-state brain connectivity measured with fMRI. Neuroimage 50:81–98 [PubMed: 20006716]

Chen A, Oathes D, Chang C, et al. (2013) Causal interactions between fronto-parietal central executive and default-mode networks in humans. Proc Natl Acad Sci 110:19944–19949 [PubMed: 24248372]

Chen B, Xu T, Zhou C, et al. (2015) Individual variability and test-retest reliability revealed by ten repeated resting-state brain scans over one month. PLoS One 10:1–21. 10.1371/journal.pone.0144963

Colclough GL, Woolrich MW, Tewarie PK, et al. (2016) How reliable are MEG resting-state connectivity metrics? Neuroimage 138:284–293. 10.1016/j.neuroimage.2016.05.070 [PubMed: 27262239]

Conde V, Tomasevic L, Akopian I, et al. (2019) The non-transcranial TMS-evoked potential is an inherent source of ambiguity in TMS-EEG studies. Neuroimage 185:300–312 [PubMed: 30347282]

David O, Cosmelli D, Friston KJ (2004) Evaluation of different measures of functional connectivity using a neural mass model. Neuroimage 21:659–673. 10.1016/j.neuroimage.2003.10.006 [PubMed: 14980568]

de Steen F, Faes L, Karahan E, et al. (2016) Critical comments on EEG sensor space dynamical connectivity analysis. Brain Topogr 1–12 [PubMed: 26492915]

Delorme A, Makeig S (2004) EEGLAB: an open source toolbox for analysis of single-trial EEG dynamics including independent component analysis. J Neurosci Methods 134:9–21 [PubMed: 15102499]

Desikan RS, Ségonne F, Fischl B, et al. (2006) An automated labeling system for subdividing the human cerebral cortex on MRI scans into gyral based regions of interest. Neuroimage 31:968–980 [PubMed: 16530430]

Draguhn A, Buzsaki G (2004) Neuronal Oscillations in Cortical Networks. Science (80-) 304:1926–1929. 10.1126/science.1099745

Engel AK, Fries P, Singer W (2001) Dynamic predictions: oscillations and synchrony in top--down processing. Nat Rev Neurosci 2:704–716 [PubMed: 11584308]

Freedberg M, Reeves JA, Hussain SJ, et al. (2019) Identifying site- and stimulation-specific TMS-evoked EEG potentials using a quantitative cosine similarity metric. bioRxiv 612499 10.1101/612499

Goldman-Rakic PS (1987) Circuitry of primate prefrontal cortex and regulation of behavior by representational memory. Handb Physiol Nerv Syst 373–417. 10.1002/cphy.cp010509

Gramfort A, Papadopoulo T, Olivi E, Clerc M (2010) OpenMEEG: opensource software for quasistatic bioelectromagnetics. Biomed Eng Online 9:45 [PubMed: 20819204]

Grefkes C, Fink GR (2011) Reorganization of cerebral networks after stroke: New insights from neuroimaging with connectivity approaches. Brain 134:1264–1276. 10.1093/brain/awr033 [PubMed: 21414995]

Greicius M (2008) Resting-state functional connectivity in neuropsychiatric disorders. Curr Opin Neurol 21:424–30. 10.1097/WCO.0b013e328306f2c5 [PubMed: 18607202]

Handwerker DA, Roopchansingh V, Gonzalez-Castillo J, Bandettini PA (2012) Periodic changes in fMRI connectivity. Neuroimage 63:1712–1719 [PubMed: 22796990]

Hauk O, Stenroos M (2014) A framework for the design of flexible cross-talk functions for spatial filtering of EEG/MEG data: DeFleCT. Hum Brain Mapp 35:1642–1653. 10.1002/hbm.22279 [PubMed: 23616402]

Hawco C, Voineskos AN, Steeves JKE, et al. (2018) Spread of activity following TMS is related to intrinsic resting connectivity to the salience network: A concurrent TMS-fMRI study. Cortex 108:160–172. 10.1016/j.cortex.2018.07.010 [PubMed: 30195825]

Hebbink J, van Blooijs D, Huiskamp G, et al. (2019) A Comparison of Evoked and Non-evoked Functional Networks. Brain Topogr 32:405–417. 10.1007/s10548-018-0692-1 [PubMed: 30523480]

Honey CJ, Honey CJ, Sporns O, et al. (2009) Predicting human resting-state functional connectivity from structural connectivity. Proc Natl Acad Sci U S A 106:2035–40. 10.1073/pnas.0811168106 [PubMed: 19188601]

Hordacre B, Moezzi B, Ridding MC (2018) Neuroplasticity and network connectivity of the motor cortex following stroke: A transcranial direct current stimulation study. Hum Brain Mapp 39:3326–3339. 10.1002/hbm.24079 [PubMed: 29655257]

Keller CJ, Bickel S, Entz L, et al. (2011) Erratum: Intrinsic functional architecture predicts electrically evoked responses in the human brain (Proceedings of the National Academy of Sciences of the United States of America (2011) 108, 25, (10308–10313) DOI: 10.1073/pnas.1019750108). Proc Natl Acad Sci U S A 108:17234 10.1073/pnas.1114425108

Lachaux J-P, Rodriguez E, Martinerie J, et al. (1999) Measuring phase synchrony in brain signals. Hum Brain Mapp 8:194–208 [PubMed: 10619414]

Lisanby SH, Gutman D, Luber B, et al. (2001) Sham TMS: Intracerebral measurement of the induced electrical field and the induction of motor-evoked potentials. Biol Psychiatry 49:460–463. 10.1016/S0006-3223(00)01110-0 [PubMed: 11274658]

Magri C, Whittingstall K, Singh V, et al. (2009) A toolbox for the fast information analysis of multiple-site LFP, EEG and spike train recordings. BMC Neurosci 10:. 10.1186/1471-2202-10-81

Mahjoory K, Nikulin VV, Botrel L, et al. (2017) Consistency of EEG source localization and connectivity estimates. Neuroimage 152:590–601. 10.1016/j.neuroimage.2017.02.076 [PubMed: 28300640]

Matsui T, Tamura K, Koyano KW, et al. (2011) Direct comparison of spontaneous functional connectivity and effective connectivity measured by intracortical microstimulation: An fMRI study in macaque monkeys. Cereb Cortex 21:2348–2356. 10.1093/cercor/bhr019 [PubMed: 21368090]

Micheloyannis S, Pachou E, Stam CJ, et al. (2006) Small-world networks and disturbed functional connectivity in schizophrenia. Schizophr Res 87:60–66. 10.1016/j.schres.2006.06.028 [PubMed: 16875801]

Nasseroleslami B, Dukic S, Broderick M, et al. (2017) Characteristic Increases in EEG Connectivity Correlate With Changes of Structural MRI in Amyotrophic Lateral Sclerosis. Cereb Cortex 1–15. 10.1093/cercor/bhx301 [PubMed: 28365777]

Nolte G, Ziehe A, Nikulin V V, et al. (2008) Robustly estimating the flow direction of information in complex physical systems. Phys Rev Lett 100:234101 [PubMed: 18643502]

O'Neill GC, Tewarie P, Vidaurre D, et al. (2017) Dynamics of large-scale electrophysiological networks: A technical review. Neuroimage 1–18. 10.1016/j.neuroimage.2017.10.003

Oostenveld R, Fries P, Maris E, Schoffelen J-MM (2011) FieldTrip: Open source software for advanced analysis of MEG, EEG, and invasive electrophysiological data. Comput Intell Neurosci 2011:. 10.1155/2011/156869

Perrin F, Pernier J, Bertrand O, Echallier JF (1989) Spherical splines for scalp potential and current density mapping. Electroencephalogr Clin Neurophysiol 72:184–187. 10.1016/0013-4694(89)90180-6 [PubMed: 2464490]

Rahman A, Reato D, Arlotti M, et al. (2013) Cellular effects of acute direct current stimulation: somatic and synaptic terminal effects. J Physiol 591:2563–78. 10.1113/jphysiol.2012.247171 [PubMed: 23478132]

Rogasch N, Zipser C, Darmani G, et al. (2019) TMS-evoked EEG potentials from prefrontal and parietal cortex: reliability, site specificity, and effects of NMDA receptor blockade. bioRxiv 480111 10.1101/480111

Rogasch NC, Thomson RH, Farzan F, et al. (2014) Removing artefacts from TMS-EEG recordings using independent component analysis: Importance for assessing prefrontal and motor cortex network properties. Neuroimage 101:425–439. 10.1016/j.neuroimage.2014.07.037 [PubMed: 25067813]

Rosenberg JR, Amjad AM, Breeze P, et al. (1989) The Fourier approach to the identification of functional coupling between neuronal spike trains. Prog Biophys Mol Biol 53:1–31 [PubMed: 2682781]

Rossi S, Hallett M, Rossini PM, et al. (2009) Safety, ethical considerations, and application guidelines for the use of transcranial magnetic stimulation in clinical practice and research. Clin Neurophysiol 120:2008–2039. 10.1016/j.clinph.2009.08.016 [PubMed: 19833552]

Sakkalis V (2011) Review of advanced techniques for the estimation of brain connectivity measured with EEG/MEG. Comput Biol Med 41:1110–1117. 10.1016/j.compbiomed.2011.06.020 [PubMed: 21794851]

Salo KST, Vaalto SMI, Mutanen TP, et al. (2018) Individual Activation Patterns after the Stimulation of Different Motor Areas: A Transcranial Magnetic Stimulation-Electroencephalography Study. Brain Connect 8:420–428. 10.1089/brain.2018.0593

Schaworonkow N, Triesch J, Ziemann U, Zrenner C (2019) EEG-triggered TMS reveals stronger brain state-dependent modulation of motor evoked potentials at weaker stimulation intensities. Brain Stimul 12:110–118. 10.1016/j.brs.2018.09.009 [PubMed: 30268710]

Seeber M, Cantonas LM, Hoevels M, et al. (2019) Subcortical electrophysiological activity is detectable with high-density EEG source imaging. Nat Commun 10:1–7. 10.1038/s41467-019-08725-w [PubMed: 30602773]

Shafi MM, Westover MB, Oberman L, et al. (2014) Modulation of EEG functional connectivity networks in subjects undergoing repetitive transcranial magnetic stimulation. Brain Topogr 27:172–191 [PubMed: 23471637]

Tadel F, Baillet S, Mosher JC, et al. (2011) Brainstorm: a user-friendly application for MEG/EEG analysis. Comput Intell Neurosci 2011:8

Tóth B, Urbán G, Háden GP, et al. (2017) Large-scale network organization of EEG functional connectivity in newborn infants. Hum Brain Mapp 38:4019–4033. 10.1002/hbm.23645 [PubMed: 28488308]

van den Heuvel MP, Hulshoff Pol HE (2010) Exploring the brain network: A review on resting-state fMRI functional connectivity. Eur Neuropsychopharmacol 20:519–534. 10.1016/j.euroneuro.2010.03.008 [PubMed: 20471808]

Vinck M, Oostenveld R, Van Wingerden M, et al. (2011) An improved index of phase-synchronization for electrophysiological data in the presence of volume-conduction, noise and sample-size bias. Neuroimage 55:1548–1565. 10.1016/j.neuroimage.2011.01.055 [PubMed: 21276857]

Vink JJJTT, Mandija S, Petrov PIPI, et al. (2018) A novel concurrent TMS-fMRI method to reveal propagation patterns of prefrontal magnetic brain stimulation. Hum Brain Mapp 39:. 10.1002/hbm.24307

Wendling F, Ansari-Asl K, Bartolomei F, Senhadji L (2009) From EEG signals to brain connectivity: A model-based evaluation of interdependence measures. J Neurosci Methods 183:9–18. 10.1016/j.jneumeth.2009.04.021 [PubMed: 19422854]

Whittingstall K, Stroink G, Gates L, et al. (2003) Effects of dipole position, orientation and noise on the occuracy of EEG source localization. Biomed Eng Online 2:1–5. 10.1186/1475-925X-2-14 [PubMed: 12605721]

Yazdan-Shahmorad A, Silversmith DB, Kharazia V, Sabes PN (2018) Targeted cortical reorganization using optogenetics in non-human primates. Elife 7:1–21. 10.7554/eLife.31034

Yeo BTT, Krienen FM, Sepulcre J, et al. (2011) The organization of the human cerebral cortex estimated by intrinsic functional connectivity. J Neurophysiol 106:1125–1165. 10.1152/jn.00338.2011. [PubMed: 21653723]

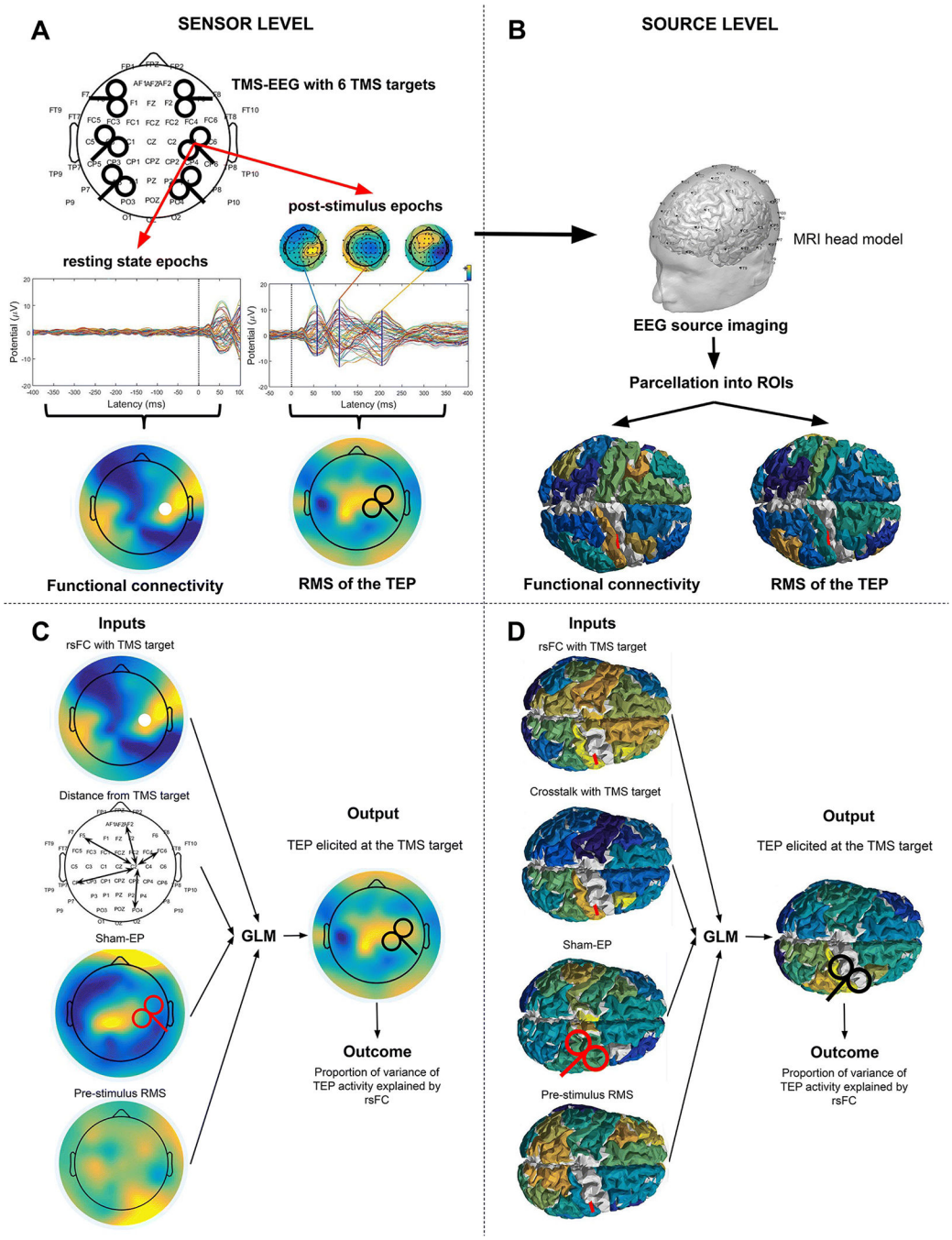

Figure 1.

Schematic overview of the analysis. **A.** TMS targets during the TMS-EEG acquisition. The DLPFC, M1 and parietal cortices of both hemispheres were stimulated. Pre-stimulus and post-stimulus epochs were obtained from the data for resting state functional connectivity analyses and TEP analysis, respectively. **B.** EEG source imaging was used for analysis in source space. **C.** Inputs and output of the GLM analysis: FC map with the TMS target as the seed region; the distance between the TMS target and the other channels; the sham-EP and the pre-stimulus RMS; An evoked activity map. The white circle illustrates the TMS target

(RM1), the red TMS coil indicates sham stimulation while the black coil indicates active stimulation. **D.** Similar inputs were used at the source level. The distance between the electrodes was replaced with crosstalk. The white circle illustrates the TMS target (RM1), the red TMS coil indicates sham stimulation while the black coil indicates active stimulation.

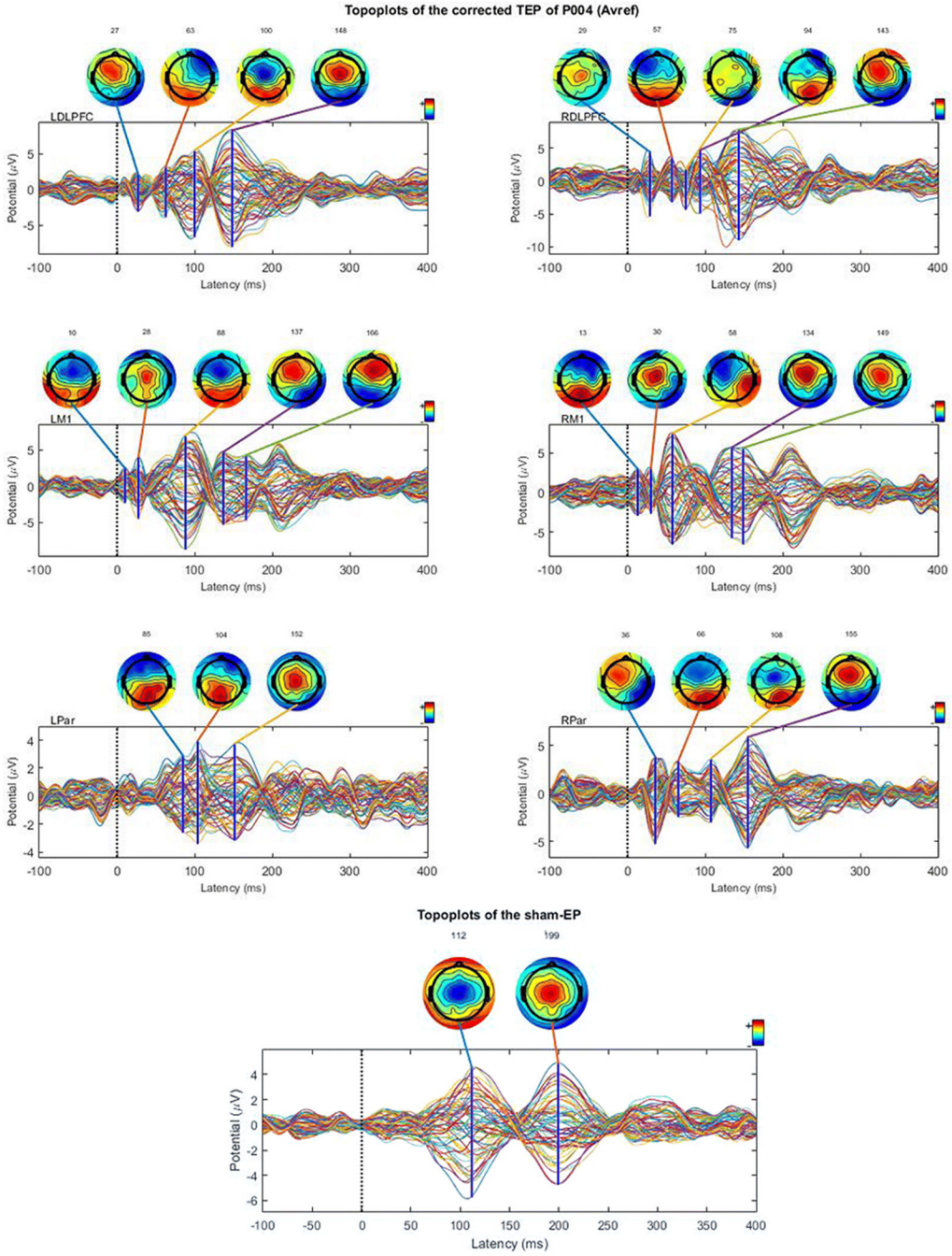

Figure 2.

Sham-corrected time series of the TEPs elicited at the 6 different stimulation sites and the sham EP are shown for a representative participant. The sham-corrected time series have been obtained by subtracting the sham-EP from the raw TEP time series. Topoplots are constructed from the time series data at different time points, which are based on peaks in the GMFP of the EP.

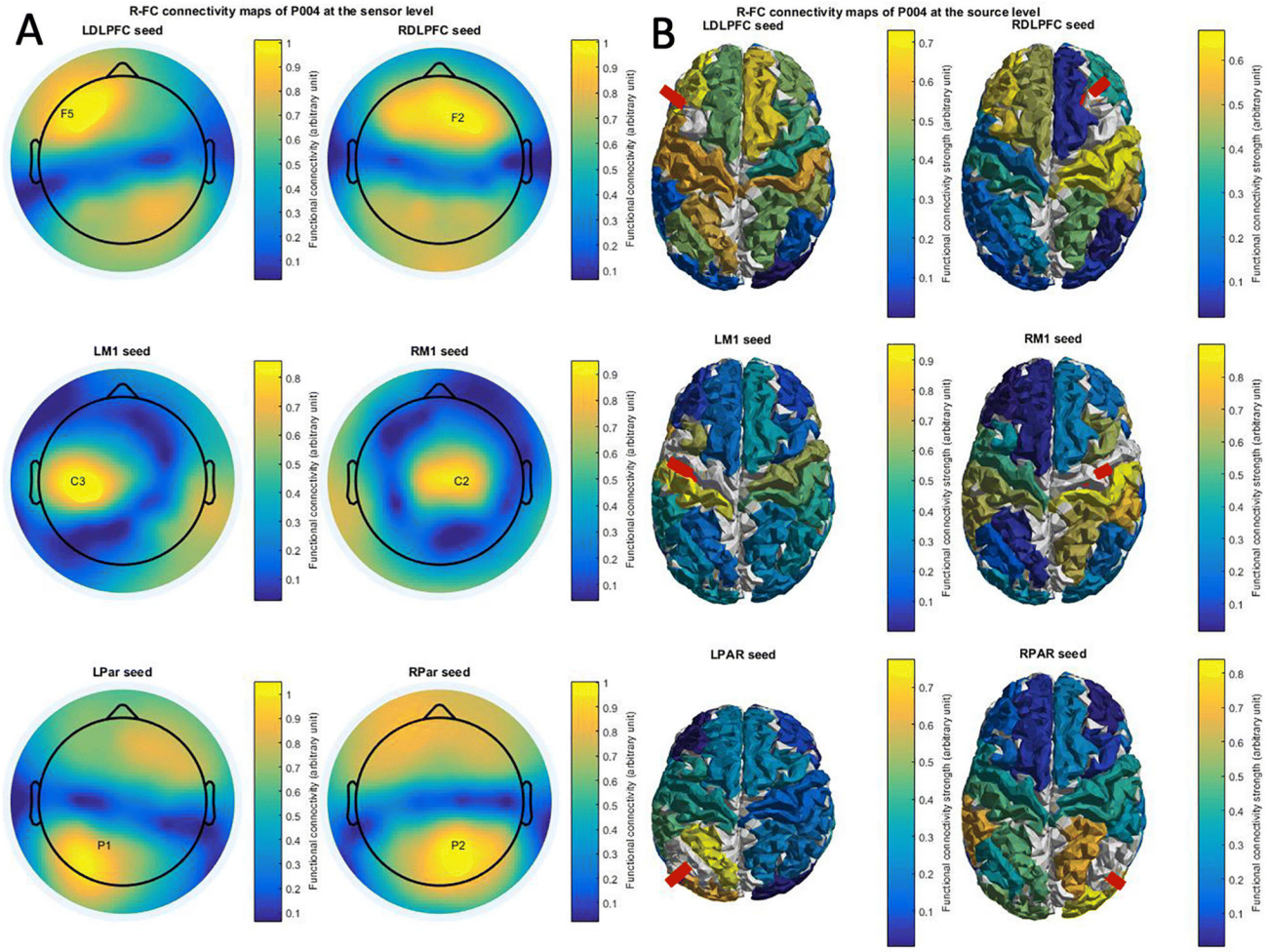

Figure 3.

Heatmaps of mean functional connectivity with different seed regions. Mean functional connectivity was averaged over multiple trials ranging from 2900 to 400ms before TMS pulse delivery. Color scales from minimum to maximum FC strength.

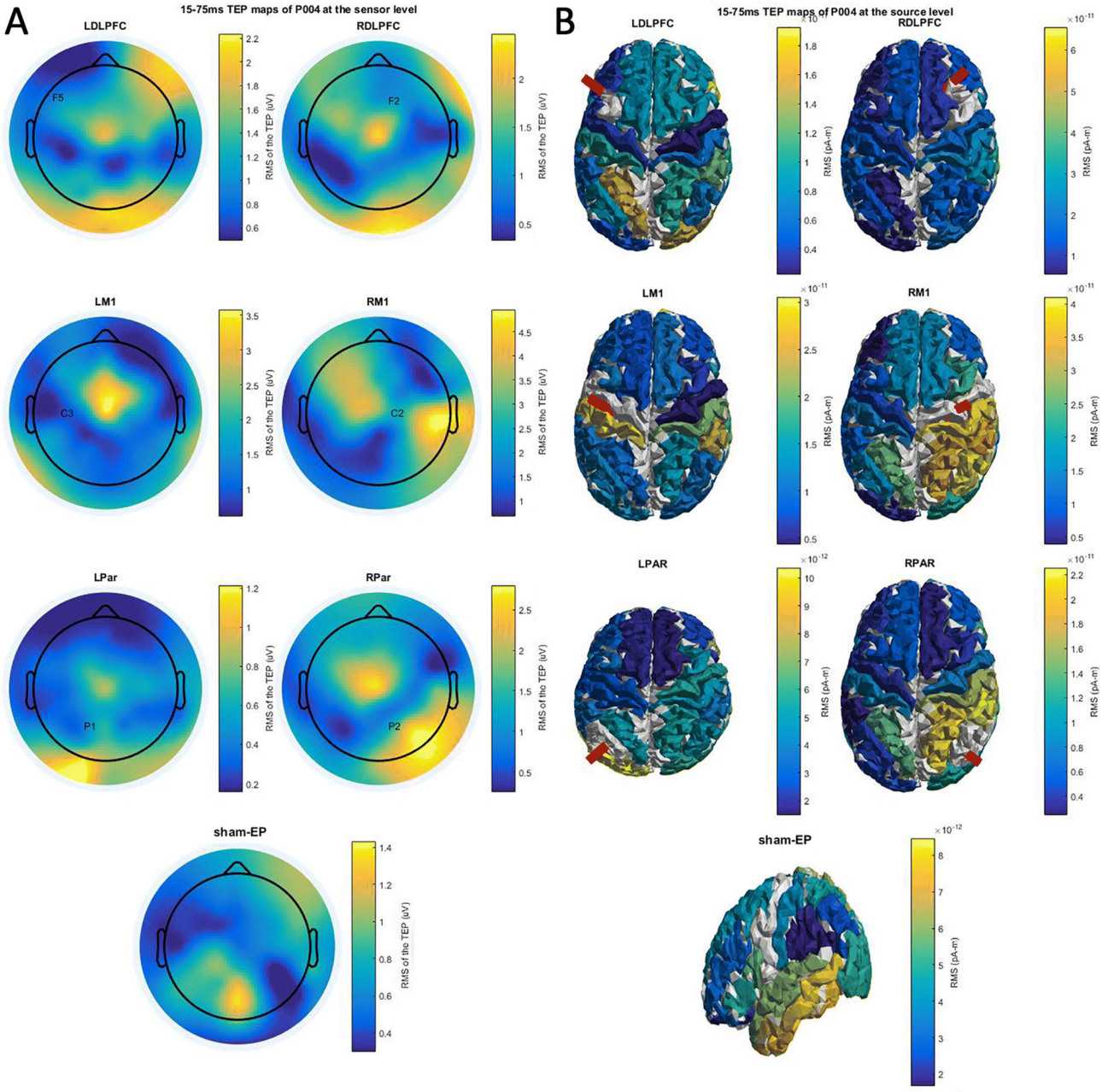

Figure 4.

Heatmaps of the spatial distribution of the TEP as determined by the RMS of the TEP over a period 15 to 75ms after TMS pulse delivery, elicited at different cortical targets. Color scales between minimum and maximum RMS.

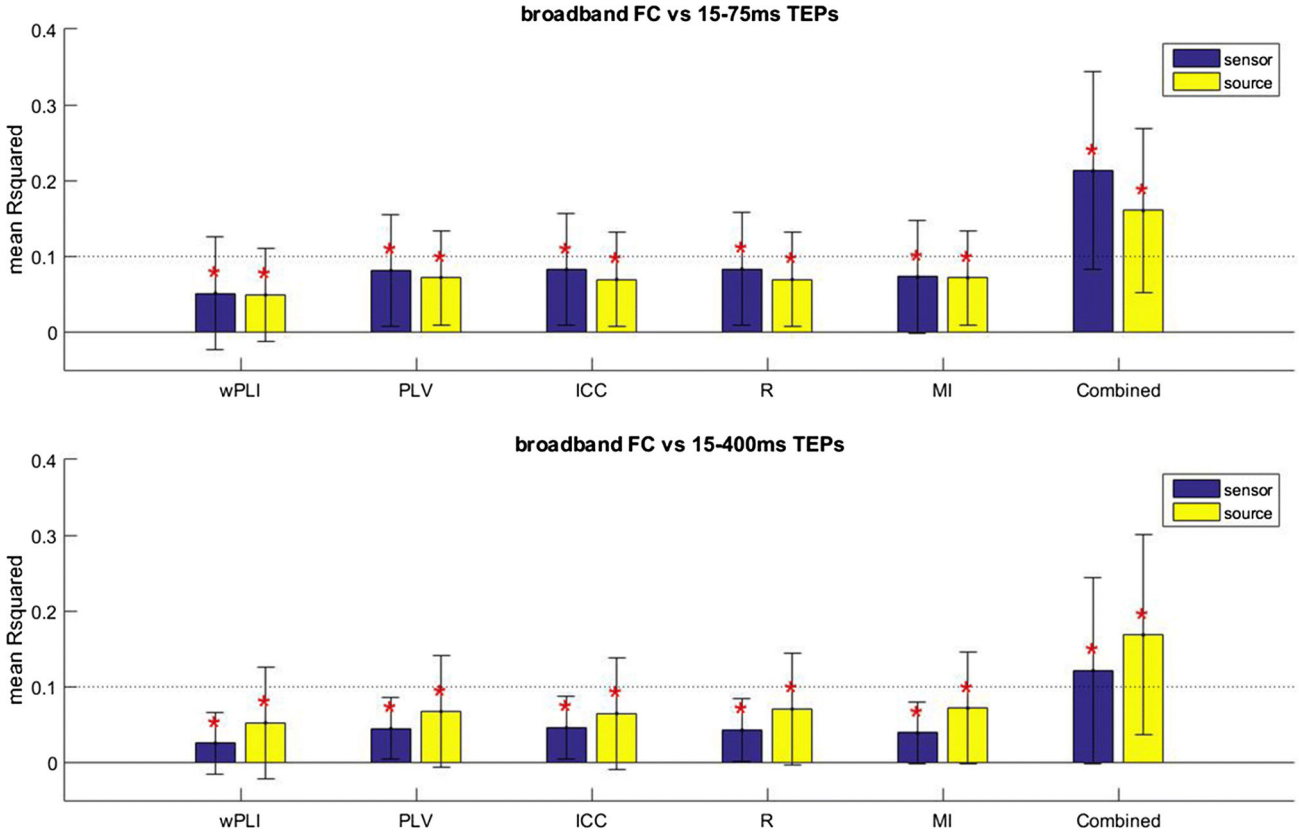

Figure 5.

Mean proportion of variance of the spatial distribution of early (15–75ms) and full (15–400ms) TEP activity explained by functional connectivity (FC) at the sensor and source level. Different FC measures are shown. The error bar indicates the standard deviation. *Significant contribution of FC ($p < 0.05$, FWE corrected).

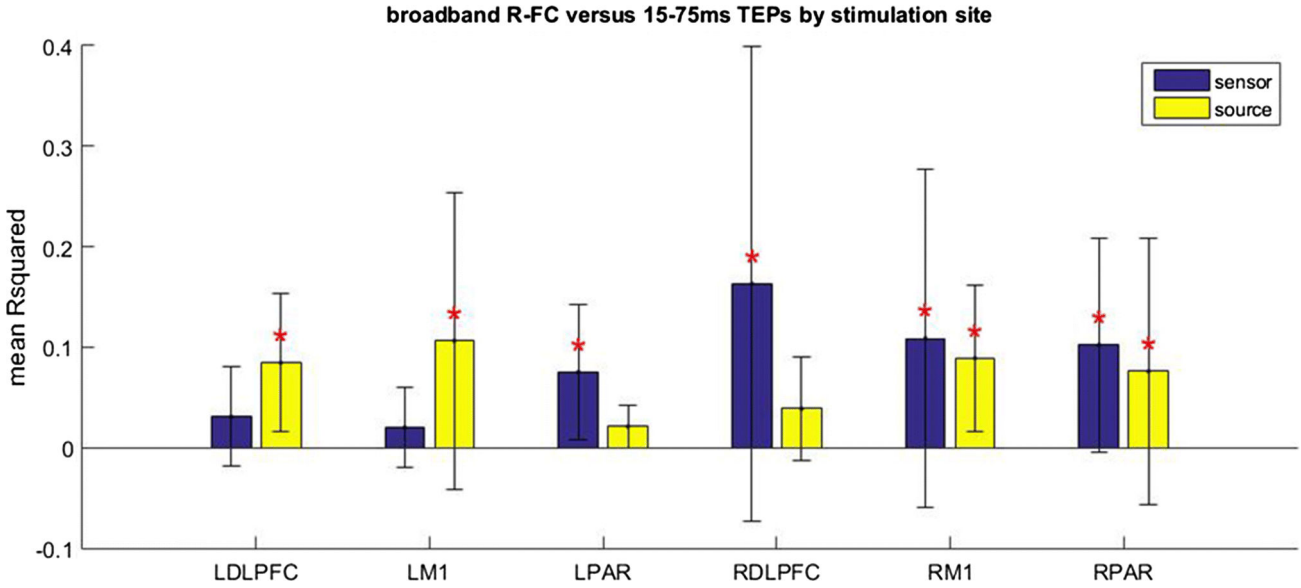

Figure 6.

Mean proportion of variance of the spatial distribution of early TEP activity explained by Pearson's correlation based FC (R-FC) at the sensor and source level for different stimulation sites. The error bar indicates the standard deviation. *Significant contribution of R-FC ($p < 0.05$, FWE corrected).

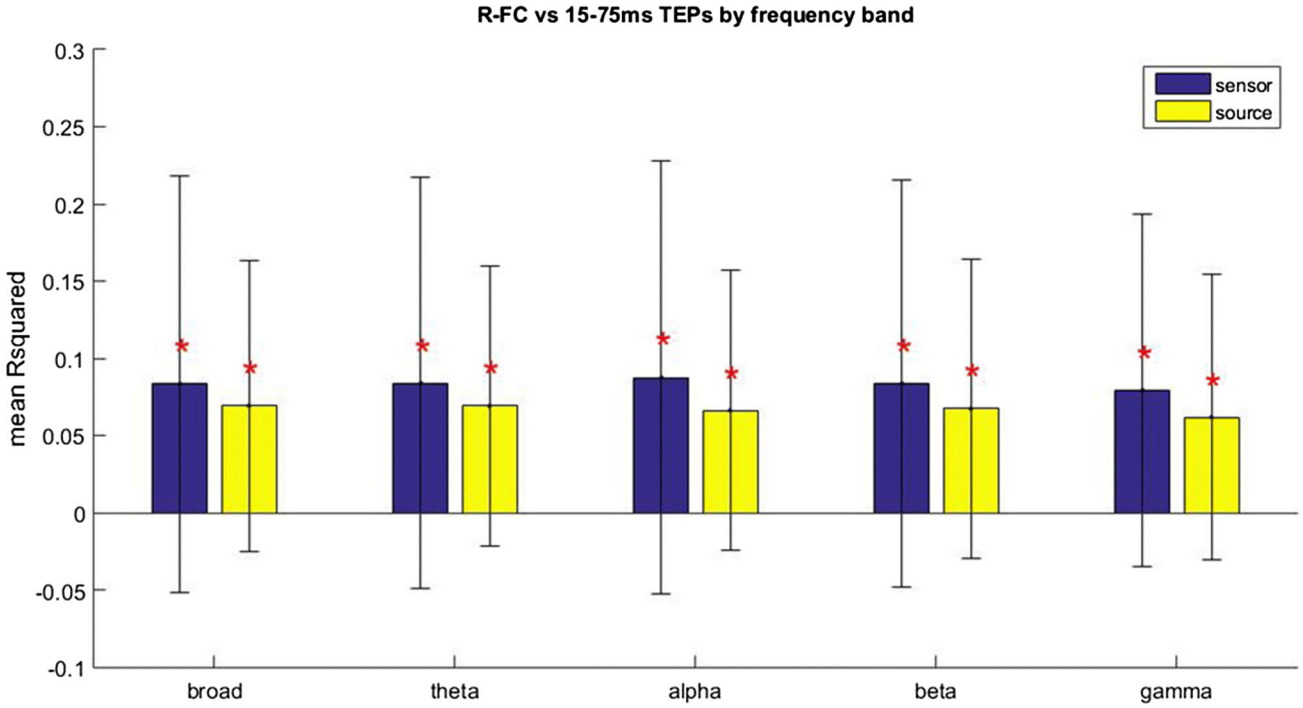

Figure 7.

Mean proportion of variance of the spatial distribution of early TEP activity explained by Pearson's correlation based FC (R-FC) at the sensor and source level for different frequency bands. The error bar indicates the standard deviation. *Significant contribution of R-FC ($p < 0.05$, FWE corrected).

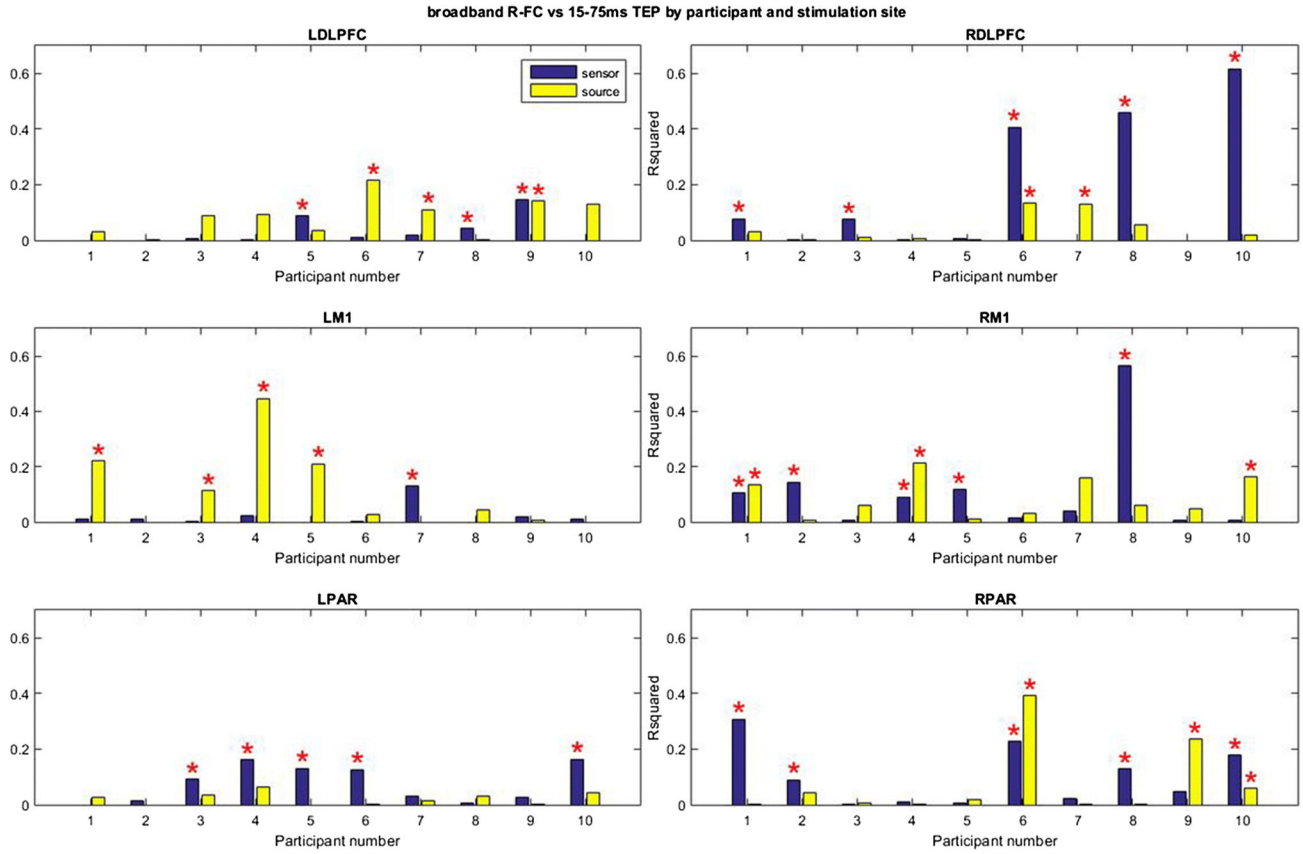

Figure 8.

Proportion of the variance of the spatial distribution of early TEP activity explained by Pearson's correlation based FC (R-FC) at the sensor and source level for individual participants. The error bar indicates the standard deviation. *Significant contribution of ICC ($p < 0.05$, uncorrected).

Table 1.

Details on connectivity and evoked activity measures.

Measure	Formula	Details
Pearson's correlation	$\rho(X,Y) = \frac{cov(X,Y)}{\sigma(X)\sigma(Y)}$	With covariance *cov* and standard deviation σ.
Mutual information	$MI(X,Y) = H(X) + H(Y) - H(X,Y)$	With entropy H.
Weighted phase lag index	$wPLI = \frac{\lvert imag(S_{xy})\rvert sgn(imag(S_{xy}))}{\lvert imag(S_{xy})\rvert}$	With cross power spectral density S_{xy}.
Coherence	$C_{xy}(\omega) = \frac{\lvert S_{xy}(\omega)\rvert^2}{S_{xx}(\omega)S_{yy}(\omega)}$	With the spectral densities S_{xx}, S_{yy} and S_{xy}.
Phase locking value	$PLV(t) = \lvert E[e^{i\Delta\varphi(t)}]\rvert$	With the expected value E and the relative phase φ.
Root mean square	$RMS = \sqrt{\frac{1}{n}\sum_i^n X_i^2}$	With the time data series X.